

A QUANTIZED ELECTRON ARRIVAL TIMES ESTIMATOR BASED DIGITAL FIBRE OPTIC RECEIVER

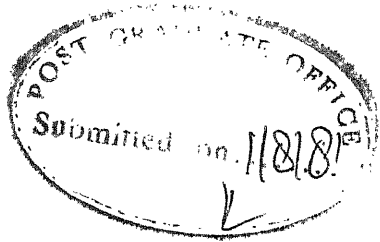
A Thesis Submitted
in Partial Fulfilment of the Requirements
for the Degree of
MASTER OF TECHNOLOGY

By
GOVIND SHARMA

to the
DEPARTMENT OF ELECTRICAL ENGINEERING
INDIAN INSTITUTE OF TECHNOLOGY, KANPUR
AUGUST, 1981

I.T. KANPUR
TRAL LIBRARY
66893
No. A

EP 1981



CERTIFICATE

Certified that the work reported in the thesis titled "A QUANTIZED ELECTRON ARRIVAL TIMES ESTIMATOR BASED DIGITAL FIBRE OPTIC RECEIVER" has been carried out under our supervision by Mr. Govind Sharma and has not been submitted elsewhere for a degree.

Rachitha

(P.K. Chatterjee)
Assistant Professor
Department of Electrical Engg.
Indian Institute of Technology,
Kanpur.

P.R.K. Rao

(P.R.K. Rao)
Professor
Department of Electrical Engg.
Indian Institute of Technology
Kanpur.

POST GRADUATE OFFICE
This thesis has been approved
for the award of the degree of
Master of Engineering (M.Tech.)
in accordance with the
regulations of the Indian
Institute of Technology Kanpur

ABSTRACT

The problem of PAM symbol detection over fibre optical digital data transmission system is considered. A sub-optimum solution is obtained under the assumptions that all past symbols have been decoded correctly, the electron emission times are quantized and signal to noise ratio is high. An upper bound on probability of error is numerically calculated using Gram-Charlier series expansion. The performance is compared with that of an 'Integrate and Dump' receiver, 'One Baud' receiver (when future symbol ISI is neglected) and an 'Ideal' receiver (in which future symbols are assumed to be known). Results are also compared with simulation studies. Timing error effects and effect of sampling rate are also considered.

ACKNOWLEDGEMENT

I would like to express my deep gratitude and thanks to Dr. P.K. Chatterjee and Dr. P.R.K. Rao for their valuable guidance and constant encouragement throughout the course of this work.

My thanks are due to more people than can be listed here; however, I would like to single out Mr. Pradeep Jain, Mr. Prabhat Mittra and Mr. S. Ramchandran for their help.

My sincere thanks to Mr. C.M. Abraham for his excellent typing.

- GOVIND SHARMA

TABLE OF CONTENTS

	Page
CHAPTER 1 INTRODUCTION	1
1.1 Organization of Thesis	2
CHAPTER 2 A MODEL FOR DIGITAL FIBRE OPTIC SYSTEM AND LITERATURE REVIEW	4
2.1 A Model for Digital Fibre Optical Communication System	4
2.2 Previous Related Work	10
CHAPTER 3 OPTIMAL AND SUB-OPTIMAL PROCESSING OF RECEIVED SIGNAL	12
3.1 Generalized Maximum Likelihood Decoding	12
3.2 Generalized Likelihood Function for Optical Fibre Detector	14
3.3 The Asymptotic ($S^2 \rightarrow \infty$) Likelihood Function	18
3.4 Likelihood Function when Electron Emission Times are Discrete	21
3.5 Decision Feedback Equalizer	24
3.6 Receiver Complexity	28
CHAPTER 4 PERFORMANCE OF THE DECISION FEEDBACK EQUALIZER	31
4.1 Gram-Charlier Series Expansion Method	32
4.2 Numerical Results	41
4.3 Simulation Results	46
4.4 Timing Error Effects	53
4.5 Effect of Sampling Rate	56
CHAPTER 5 CONCLUSION	60
REFERENCES	63

CHAPTER 1

INTRODUCTION

A large part of traditional communication system practice is directed to detecting and processing electrical signals received over diverse time-continuous communication channels. The physical realization of each of these traditional systems has led to mathematical treatment designed to handle problems such as linear distortion or fading, which were peculiar to one or even several such systems. But the principal concern of mathematical treatment of these time-continuous channels has been the ubiquitous additive Gaussian noise. In fact, it would be fair to say that much of the structure of the mathematical treatment used has been dictated by the mathematical properties of this noise. In the absence of noise, many problems would immediately degenerate, at least theoretically, to situations of perfect detection, infinite capacity etc.

The consideration of some promising optical communication systems seems to alter the above picture. Here, we have in mind the transmission of information by way of light pulses propagating through an optical fibre and subsequently detected by a photo-detector that converts electromagnetic energy in the fibre to electrical signals in a circuit. We immediately note certain features which

this problem has in common with the traditional problems. For one thing, the fibre can delay, attenuate or spread the transmitted pulses. For another, the electrical signal after photo-detection may be corrupted by additive Gaussian noise. Yet there is another fundamental impairment. The received intensity of the electromagnetic signal that propagates in the fibre (which acts as a waveguide) is, under practical conditions, sufficiently weak. And any effective scheme of detection of the signal must take into account the quantum nature of the electromagnetic disturbance. In other words, the detection mechanism must be based upon photon counting. Here, a new element enters the problem: photon counting is subject to statistical fluctuations. In the quantum case, a signal uncorrupted by any external disturbance still carries with it, its own 'noise', as it were, which is not Gaussian. This noise, described as an electron counting process, is a time-varying Poisson process whose intensity (or rate) function $\lambda(t)$ varies in direct proportion to the information-bearing pulse train.

This thesis is devoted to a study of determining a receiver structure for the above mentioned situation and evaluating its performance.

1.1 ORGANISATION OF THE THESIS

The thesis comprises 5 chapters. Chapter 2, after

introducing a mathematical model for the fibre optical communication system, briefly describes the various techniques proposed in the relevant literature, for data transmission over the optical fibre.

In Chapter 3 a receiver structure is derived and a hardware block schematic for the receiver is presented. This is followed by a discussion on the complexity of the proposed receiver.

In Chapter 4 the performance of the proposed equalizer is analysed and it is compared with that of an 'Integrate and Dump' receiver, 'One Baud' receiver (where future symbol ISI is neglected) and 'Ideal' receiver (in which future symbols are also assumed to be known). Some simulation results are also presented.

Chapter 5 concludes this thesis, describing some shortcomings of the present work, and suggests approaches for further work to refine the receiver described herein.

CHAPTER 2

A MODEL FOR DIGITAL FIBRE OPTIC SYSTEM AND LITERATURE REVIEW

In this chapter, first we present a mathematical model of a typical fibre optical communication system. Then we formulate the optical detection problem. After this we describe the previous work done to solve this problem.

2.1 A MODEL FOR DIGITAL FIBRE OPTICAL COMMUNICATION SYSTEM

Here we consider the binary pulse amplitude modulated (PAM) transmission system. Here the choice between a 'one' or a 'zero' is translated into the presence or absence of a short burst of optical power (light) in the fibre. To understand this in more detail, we shall trace the passage of a single pulse through the mathematical model of our system (see Fig. 2.1). In case of an 'one' being transmitted, an electric pulse (a pulse of duration T) turns on a 'flash light', which in this case is a laser or light-emitting diode, and electromagnetic energy is sent into the transmission medium (optical fibre). In Fig. 2.1 we have shown how this pulse spreads as it travels along the fibre. Fig. 2.2 shows some of the typical pulse responses of the fibre optical system. These curves are taken from Cartledge [3]. There are two courses open to us when this pulse reaches the other end of fibre. First, we can process

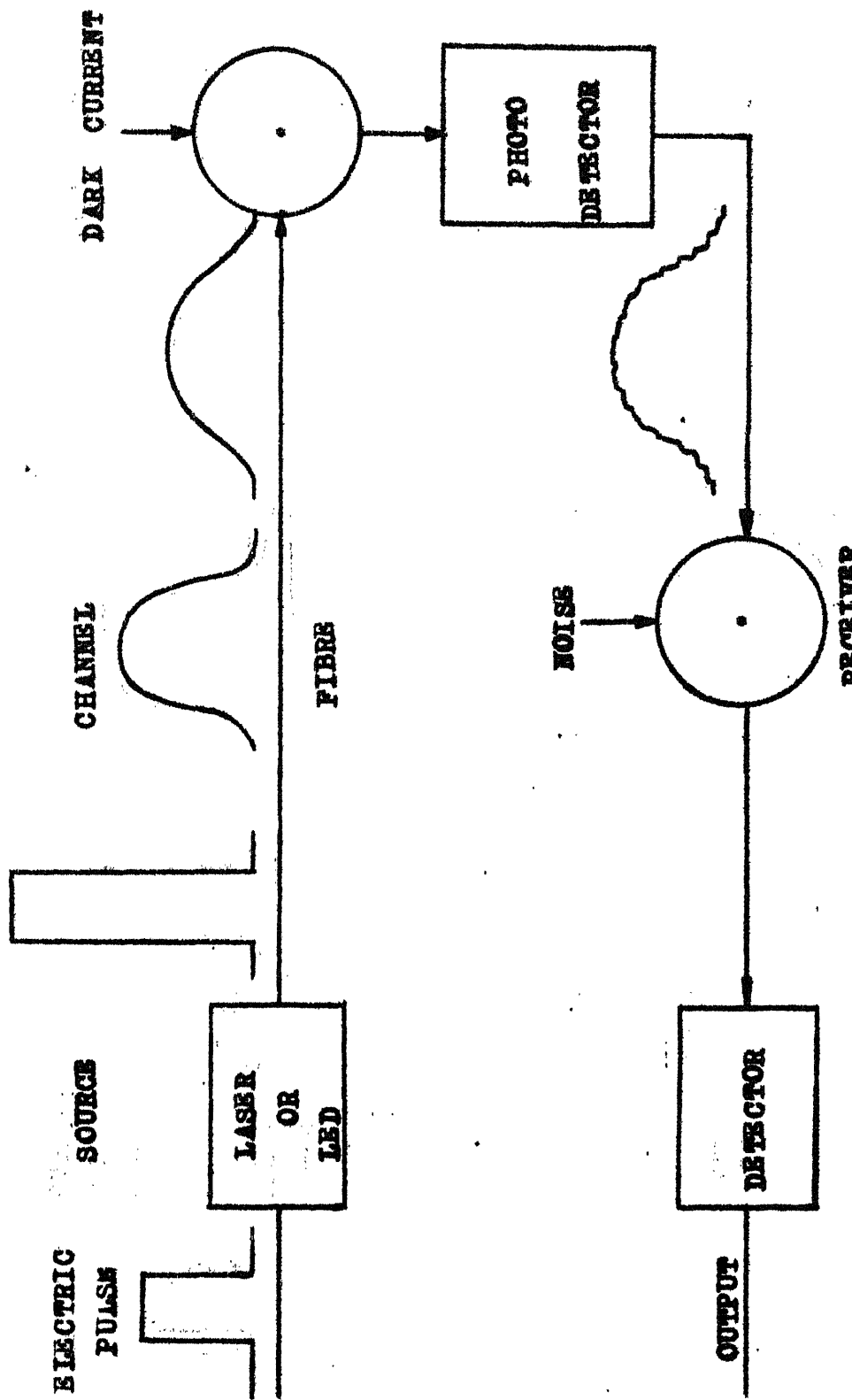


Fig. 2.1. OPTICAL COMMUNICATION SYSTEM MODEL

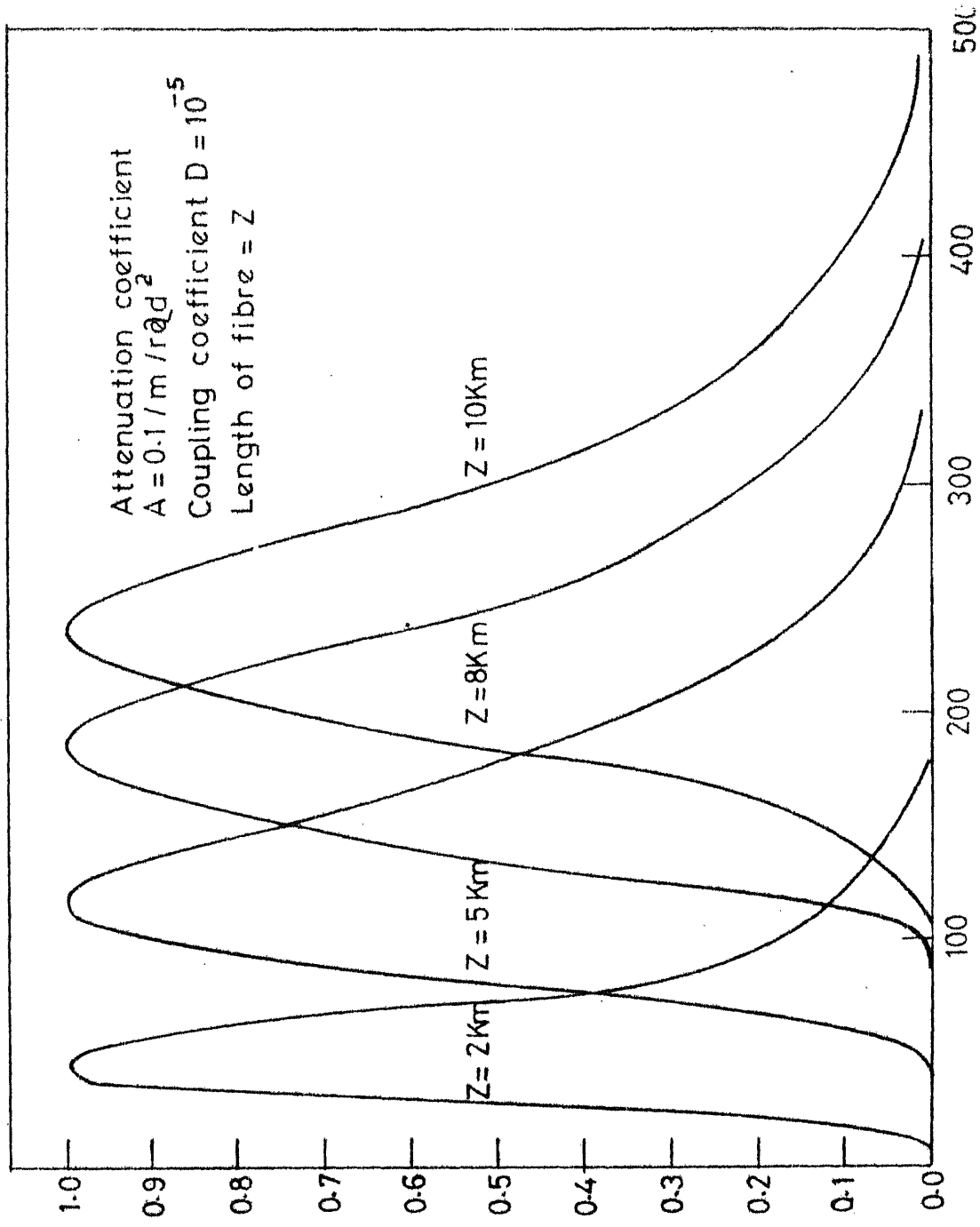


FIG. 2.2 IMPULSE RESPONSE

the received electromagnetic field dictated by quantum mechanical considerations [4]. But such schemes of processing are complex. Instead, we adopt a practical approach and assume that a direct detection is used to convert optical energy to an electrical signal. This is accomplished by using a photodetector prior to any signal processing. The electrons will be emitted due to the electromagnetic energy falling on the detector. Exactly when in time the electrons are emitted is random and is the Poisson process mentioned earlier. The probability of receiving a count between time t and $t+dt$ is proportional to $p(t)dt$, where, owing to effects in the fibre, $p(t)$ is a distorted and attenuated version of the transmitted pulse (see Fig. 2.2). In practice a background of counts also exists. This is called the dark current and is modelled by introducing a constant additive intensity function λ_0 before the detector, although some of these counts can originate in the physical detector itself. Typically, transmitted power and transmission loss (fibre length) are adjusted so that, of the order of one to two hundred photons per pulse are, on the average, detected. The dark current contributes about 1 to 5 percent of counts.

To transmit a 'zero', we simply do not turn on the transmitting power, and detector only registers counts resulting from the dark current.

We have been loosely speaking of the output of the photo-detector as 'counts'. The actual current at the output of this device caused by a photon is a wide-band pulse $g \cdot w(t)$ (very narrow compared to T , a delta function in the limit), where g is an integer valued random variable or $g \equiv 1$, depending on whether or not an avalanche diode issued. The electric current at the output of the photo-detector is further distorted by Gaussian noise whose effects are of lesser importance when an avalanche diode is used but not for the case when $g \equiv 1$. The pulse energy-to-noise ratio, $\int w^2(t)dt/N_0$, is typically -20 dB. In other words, the response of the photodetector to an individual photon is masked by the additive back ground noise. This is in contrast to the photomultiplier and avalanche photodiode whose mean gain \bar{g} and mean square gain \bar{g}^2 can be rather large. For these devices the average pulse-energy-to-noise ratio, $\bar{g}^2 \int w^2(t)dt/N_0$, can be of the order of 20 dB.

By invoking the principle of superposition for optical fibre transmission (as shown by Personick [5]) we can extend our single pulse description to obtain a model for transmission of an entire pulse train. Thus, if we transmit a sequence of on or off pulses, the photo-detector output $r(t)$, can be written as

$$r(t) = \sum_k g_k w(t-t_k) + n(t) \quad (2.1)$$

where the time instants t_k form a Poisson process having intensity $\lambda(t)$, with

$$\lambda(t) = \sum_1 a_1 p(t-1T) + \lambda_0 \quad (2.2)$$

where

$p(t) \geq 0$ is pulse response of fibre (2.3)

$a_1 = 0, 1$ are equiprobable data symbols

$\lambda_0 \geq 0$ is dark current

T is signalling interval

$n(t)$ is an additive noise process

g_k is avalanche gain factor

$w(t)$ is output pulse of photodetector.

The number k of photon arrivals is random whose probability distribution is given by

$$\text{prob}(k = K) = \frac{\lambda^K e^{-\lambda}}{K!} \quad (2.4)$$

where

$$\lambda = \int_0^\tau \lambda(t) dt \quad (2.5)$$

is the average number of photon arrival in the interval 0 to τ .

The subject of our investigation is : How should the photo-detector output $r(t) = I(t) + n(t)$ be processed so as to minimize the probability of error?

Before answering this question in the next chapter, we briefly describe some of the previous work in the related field.

2.2 PREVIOUS RELATED WORK

In the past few years a useful communication theoretic model for data transmission over the fibre optical channels has evolved. Bar-David [6] and Gagliardi and Karp [7] have considered the optimal reception problem in the absence of dispersion (Inter symbol interference) and additive noise. Bar-David has considered the situation when the additive noise is also not present. The maximum likelihood function derived by him requires the knowledge of the electron emission instants. The receiver obtained is a weighted photon counter. If the output pulses are narrow enough to be considered as delta functions then this can be replaced by a linear filter with impulse response.

$$h(-t) = \ln(\lambda_1(t)/\lambda_0(t)) \quad (2.6)$$

and optimum threshold is given as

$$F = \int \lambda_1(t) dt - \int \lambda_0(t) dt \quad (2.7)$$

Gagliardi and Karp have considered the problem of M-ary Poisson detection in a back ground of additive Poisson noise.

Personick [8] has considered the detection problem in the presence of thermal noise and intersymbol interference. He presents a linear sub-optimum solution. He gives the design of a front-end amplifier to take into account precisely the input pulse shape and equalizer filter shape. The output pulse shape after equalization is assumed to be a full raised -cosine waveform.

Other sub-optimal receivers in the presence of noise and ISI are considered by Messerschmitt [9]. The receiver minimizes the mean square error (MSE), both for linear as well as decision feedback equalizers. The receiver is derived assuming the structure to be a linear filter followed by a forward and a backward tapped delay line. Receiver performance in terms of probability of error has not been evaluated.

The ML detection has been considered by Foschini et al. [10]. The receiver obtained consists of two Viterbi-decoders in cascade.. Some of the relevant details of this receiver are presented in the next chapter where a modification of the same is considered.

CHAPTER 3

OPTIMAL AND SUB-OPTIMAL PROCESSING OF RECEIVED SIGNAL

In this chapter we begin to answer the question posed at the end of section 2.1 (How to optimally process the photodetector output?) by presenting a derivation of the likelihood function associated with the received signal. The likelihood function so obtained is too complicated to yield a useful receiver. Under the assumptions of a high signal to noise ratio as obtains when an avalanche photodiode or a photo-multiplier tube is used, and quantized time instants of electron emissions, following [10], we show that the optimal receiver consists of two Viterbi decoders in cascade. As hardware implementation of a Viterbi decoder at high data rates, with existing technologies, is nearly ruled out, in this thesis we consider a modification of the likelihood function to obtain a decision feedback equalizer.

3.1 GENERALIZED MAXIMUM LIKELIHOOD DECODING

In the digital system of Fig. 2.1, the decoder has the task of observing the detector output and decoding the transmitted signal. The presence of added noise fields during photodetection, along with the added system noise prior to decoding circuitry, causes errors in the bit decisions made. An accepted procedure for decoder design for generating these

decisions makes use of the concept of Maximum Likelihood (ML) test. Under this criterion, the decoder upon observing the noisy detector output, selects the bits that have the highest probability of causing this output. Mathematically, this requires the decoder to compute conditional probabilities $p(r(t)|i)$ (called likelihood functions) for each combination of bits over τ sec (τ sec is observation interval), and select the maximum. The decoder computes

$$L_i = p(r(t)|i) = \text{the probability of receiving } r(t) \text{ given } i \text{th intensity was received} \quad (3.1)$$

for each i and selects the maximum.

For equally likely intensities the ML test is equivalent to MAP (maximum a posteriori) test in which the detector selects the intensity, which has the highest probability of having been sent, as the received intensity. A MAP detector is a minimum probability of error detector. Since for equally likely intensities ML test is same as MAP test, it is also a minimum probability of error criterion.

If the received signal intensity happens to depend upon a random parameter θ , having apriori density $p(\theta)$, then the previous discussion is still valid, provided that we remember that $p(r(t)|i)$ is a conditional average over θ [2]. That is we use $p(r(t)|i) = E_{\theta} p(r(t)|i,\theta)$, where $p(r(t)|i,\theta)$ is the probability conditioned on the i th intensity being

received with parameter value θ . Thus likelihood function becomes

$$L_i = \int p(r)(t) | i, \theta \quad p(\theta) d\theta \quad (3.2)$$

This is called a generalized likelihood function. This concept can be generalized for several random parameters.

3.2 GENERALIZED LIKELIHOOD FUNCTION FOR OPTICAL FIBRE DETECTOR

If we denote the received signal by

$$r(t) = I_m(t) + n(t) \quad (3.3)$$

where $I_m(t)$ is the information carrying filtered Poisson process

$$I_m(t) = \sum_{j=1}^{k(t)} g_j w(t-t_j) \quad (3.4)$$

and where index m (corresponding to $\lambda_m(t)$) is hidden in the statistics of $\{t_i\}$ and $k(t)$. These statistics are described by equations (2.2) to (2.4) with $\lambda(t)$ replaced by $\lambda_m(t)$.

As we have mentioned earlier, the random variables $\{g_n\}$ represent the random gains & $w(t)$ is the pulse shape due to emission of an electron. In actual practice the additive noise at the output of the detector is not white but it can be whitened by a filter before additional processing. The effect of this filter and pulse shape due to emission of an

electron can be combined together, then $w(t)$ is this resultant pulse shape.

The likelihood function conditioned on $I_m(t)$ has the standard form [2]

$$L_m(r(t) | I_m) = \exp\left(\frac{1}{N_0} \int_0^{\tau} I_m(t) r(t) dt - \frac{1}{2N_0} \int_0^{\tau} I_m^2(t) dt\right) \quad (3.5)$$

The desired likelihood function is the expectation of (3.5) with respect to $I_m(t)$ for fixed m , i.e.

$$L_m(r(t)) = E_{I_m}(L_m(r(t) | I_m)) \quad (3.6)$$

Once the intensity $\lambda_m(t)$ is specified, the above expectation is taken with respect to the number of arrivals, the arrival times and the avalanche gain values. The detailed evaluation of this expectation and the interpretation of the resulting structure in terms of simple physical operations on $r(t)$, are our objectives. The exact structure turns out to be so complex that many judicious approximations will have to be made to glean the essential nature of the operations.

Neglecting the edge effects on the integrals and assuming that the observation time τ is much larger than the effective duration of a single pulse $w(t)$, we can express the inner product and square term indicated in (3.5) as

$$\int_0^{\tau} I_m(t) r(t) dt = \sum_{j=1}^k g_j P(t_j) \quad (3.7)$$

where

$$P(t_j) = \int_0^{\tau} w(t-t_j) r(t) dt \quad (3.8)$$

The square term is written as

$$\int_0^{\tau} I_m^2(t) dt = \sum_{j=1}^k \sum_{l=1}^k g_j g_l R(t_j - t_l) \quad (3.9)$$

where

$$R(t) = \int_0^{\tau} w(u) w(t-u) du \quad (3.10)$$

is the pulse correlation function.

Substituting (3.7) and (3.9) into (3.5) and (3.6), we obtain

$$L_m(r(t)) = E_I \left[\exp \left(\frac{1}{N_0} \sum_{j=1}^k g_j P(t_j) - \frac{1}{2N_0} \sum_{j,l=1}^k g_j g_l R(t_j - t_l) \right) \right] \quad (3.11)$$

Employing the vector notation

$$\underline{g_k} = (g_1, g_2, \dots, g_k) \quad \text{and}$$

$\underline{t_k} = (t_1, t_2, \dots, t_k)$ gives the expression

$$L_m(r(t)) = E_{\underline{t_k}, \underline{g_k}, k} \left[\exp \left(\frac{1}{N_0} \sum_{j=1}^k g_j P(t_j) - \frac{1}{2N_0} \sum_{j,l=1}^k g_j g_l R(t_j - t_l) \right) \right] \quad (3.12)$$

The joint density $p(t_1, t_2, \dots, t_n, n)$ is given as (see [1], p. 111)

$$p(t_1, t_2, \dots, t_n, n) = \frac{1}{n!} \prod_{j=1}^n \lambda(t_j) \exp \left(- \int_0^{\tau} \lambda(t) dt \right) \quad (3.13)$$

After performing the expectation in (3.12) using (3.13), we obtain for the likelihood function

$$L_m(r(t)) = \exp(-\Lambda_m(\tau)) \sum_{n=0}^{\infty} \frac{1}{n!} \sum_{g_n} \int_0^\tau dt_n \prod_{j=1}^n \lambda_m(t_j) p_G(g_j) \cdot \\ \exp\left(\frac{1}{N_o} \sum_{j=1}^n g_j P(t_j) - \frac{1}{2N_o} \sum_{j,l=1}^n g_j g_l R(t_j - t_l)\right) \quad (3.14)$$

where $p_G(g_j)$ is the discrete probability density function of the avalanche gain and where it is understood that when $n = 0$, the summand is taken to be unity.

By suitably normalizing the likelihood function, (3.14), $\frac{1}{N_o}$ can be replaced by the pulse signal-to-noise ratio. The normalization entails replacing $R(t)$ by $R(t)/R(0)$, $P(t_j)$ by $P(t_j)/R(0)$ \bar{g} and g_k by g_k/\bar{g} ; consequently

$$S^2 = \bar{g}^2 R(0)/N_o \quad (3.15)$$

and may be viewed as an average pulse signal-to-noise ratio. Depending upon the presence or absence of avalanche gain, S^2 is either large or small. To save on notation we still represent $R(t)/R(0)$, g_k/\bar{g} and $P(t_j)/R(0)\bar{g}$ as $R(t)$, g_k and $P(t_j)$ respectively. Presence of S^2 in expression will indicate that we are using the normalized quantities. Now the likelihood function becomes

$$L_m(r(t)) = \exp(-\Lambda(\tau)) \sum_{n=0}^{\infty} \frac{1}{n!} \sum_{g_n} \int_0^\tau dt_n \prod_{j=1}^n \lambda_m(t_j) p_G(g_j) \cdot \\ \cdot \exp\left[S^2 \left(\sum_{j=1}^n g_j P(t_j) - \gamma_2 \sum_{j,l=1}^n g_j g_l R(t_j - t_l)\right)\right] \quad (3.16)$$

We see that the likelihood function given in (3.16) is too complicated to be interpreted and to be implemented. In the presence of avalanche gains, the average signal to noise ratio, S^2 , is large. This implies that the photon arrival times can be accurately estimated and these estimates can then be used to aid the detector in making accurate decisions. Heuristically, the receiver attempts to "whiten" or peak up the pulse $w(t)$. The presence of Gaussian noise, however small, prevents pulse whitening via linear filtering. The nonlinear manner in which the receiver estimates the arrival times is of our interest and will be presented in the sequel.

3.3 THE ASYMPTOTIC ($S^2 \rightarrow \infty$) LIKELIHOOD FUNCTION

In this section, the basic idea is to asymptotically evaluate the multiple sums or integrals. When $S^2 \rightarrow \infty$, the $2n$ -fold integrals appearing in the likelihood function (3.16) become increasingly sensitive to the value of the exponent, and in the limit the integral is completely determined by the coordinates that maximize the exponent. This statement is made precise by the multi-dimensional version of Laplace Theorem [1] which gives for each n

$$\begin{aligned}
 & \lim_{S \rightarrow \infty} \int_0^{\mathcal{T}} dt^n \sum_{g_n} \prod_{j=1}^n p_G(g_j) \lambda(t_j) \exp \left[S^2 \left(\sum_{j=1}^n g_j P(t_j) - \right. \right. \\
 & \quad \left. \left. \gamma_2 \sum_{j,l}^n g_j g_l R(t_j - t_l) \right) \right] \\
 & \sim \prod_{j=1}^n p_G(g_j^*) \lambda(t_j^*) \exp \left[S^2 \left(\sum_{j=1}^n g_j^* P(t_j^*) - \right. \right. \\
 & \quad \left. \left. \gamma_2 \sum_{j,l}^n g_j^* g_l^* R(t_j^* - t_l^*) \right) \right] \tag{3.17}
 \end{aligned}$$

where $(t_1^*, t_2^*, \dots, t_n^*)$ and

$$\begin{aligned}
 & (g_1^*, g_2^*, \dots, g_n^*) \text{ maximize the exponent} \\
 & \sum_{j=1}^n g_j P(t_j) - \gamma_2 \sum_{j,l}^n g_j g_l R(t_j - t_l) \tag{3.18}
 \end{aligned}$$

under the constraints $0 \leq t_i \leq \mathcal{T}$, $i = 1, 2, \dots, n$.

The determination of extremizing values of $\{t_j^*\}$ and $\{g_j^*\}$ appear very difficult. For the time being let us assume that these sets are determined somehow. Rewriting right hand side of (3.17) as

$$\begin{aligned}
 & \prod_{j=1}^n p_G(g_j^*) \lambda(t_j^*) \exp \left[S^2 \left(\sum_{j=1}^n g_j^* P(t_j^*) - \right. \right. \\
 & \quad \left. \left. \gamma_2 \sum_{j,l}^n g_j^* g_l^* R(t_j^* - t_l^*) \right) \right] = C_n(\mathcal{T}) \exp(S^2 B_n(\mathcal{T})) \tag{3.19}
 \end{aligned}$$

where we have indicated the dependence of both the coefficients and exponent on the observation interval \mathcal{T} . Using (3.16), (3.17) and (3.19) we get the Dirichlet series

$$L_m(r(t)) \sim \exp(-\int_0^T \lambda_m(t) dt) \sum_{n=0}^{\infty} C_n(T) \exp(S^2 B_n(T)) \quad (3.20)$$

As $S \rightarrow \infty$, it is well known that the Dirichlet series is dominated by the term with the largest exponent, i.e.,

$$\lim_{S \rightarrow \infty} L_m(r(t)) \sim \exp(-\lambda_m) C_n^*(T) \exp(S^2 B_n^*(T)) \quad (3.21)$$

where $B_n^*(T)$ is the largest exponent. We see that n^* is an estimate of the number of Poisson events occurring in the interval T and that $t_1^*, t_2^*, \dots, t_{n^*}^*$ are estimates of these occurrence times, while $g_1^*, g_2^*, \dots, g_{n^*}^*$ are estimates of avalanche gains. Since neither the exponent in (3.21) nor the term $\prod_{j=1}^{n^*} p_G(g_j^*)$ in $C_n^*(T)$ is hypothesis sensitive,

the relevant portion of the likelihood function is

$$L_m(r(t)) \sim \exp(-\lambda_m) \prod_{j=1}^{n^*} \lambda(t_j^*) \quad (3.22)$$

where n^* is the number of time points that maximize the exponent of (3.20) and $\{t_j^*\}$ are the values of these time points. We note here that likelihood function given in (3.22) is same as the likelihood function derived by Bar-David [6] where he assumes that arrival times of photon are known exactly.

Once the exponent is jointly optimized with respect to t_n and g_n the estimates of the avalanche gain is not utilized further. This is so because the avalanche gain is a property of the photo-diode and conveys no information concerning the intensities.

As we have seen earlier that evaluation of (3.17) is a difficult task. It becomes simpler if we assume that the electron emissions are discrete. This we do in the next section.

3.4 LIKELIHOOD FUNCTION WHEN ELECTRON EMISSION TIMES ARE DISCRETE

We assume that photons are constrained to arrive at discrete instants $j\Delta$ ($j=1, 2, \dots, J = \frac{\tau}{\Delta}$). This gives rise to the discrete likelihood function

$$L_m(r(t)) = \exp(-\Lambda_m(\tau)) \sum_{n=0}^{\infty} \frac{1}{n!} \sum_{t_n} \sum_{g_n} \prod_{j=1}^n \lambda(t_j) p_G(g_j) \cdot \\ \cdot \exp \left[s^2 \left(\sum_{j=1}^n g_j P(t_j) - \gamma_2 \sum_{jl} g_j g_l R(t_j - t_l) \right) \right] \quad (3.23)$$

where $\{t_j\}$ can take value $j\Delta$, ($j = 1, 2, \dots, J$). Using the same reasoning as before we will get expressions similar to (3.17) - (3.22), where expressions will contain summations instead of integrals. We choose the time quantization interval Δ small enough to ensure that the probability of more than one electron emission occurring in a time interval Δ is vanishingly small under each hypothesis $\lambda_m(t)$ (effect of varying Δ is discussed in next chapter, Sec. 4.5). In this frame-work, the set of time points $\{t_k^*\}$, specifies J -points in the interval $(0, \tau)$, and the exponent can be written as

$$\sum_{j=1}^n g_j P(t_j) - \gamma/2 \sum_{j,l=1}^n g_j g_l R(t_j - t_l) = \\ - \sum_{i=1}^J g_j q_j P(j\Delta) - \gamma/2 \sum_{i,l=1}^J g_j q_j g_l q_l R(\Delta j - \Delta l) \quad (3.24)$$

where $q_j = 0, 1$ depending upon the photon arrival interval $j\Delta$. It is clear that the product $g_j q_j$ is inseparable in the optimization of (3.24). Once the optimum values of g_j and q_j are determined, only the values of q_j play a further role in the detection procedure. Keeping this in mind we let

$b_j = g_j q_j$, where b_j will range over the allowable values of g_j as well as zero. For convenience sake we call this discrete set B . Then, the optimization problem posed in (3.18) and (3.21),

$$\max_{\substack{g_n, t_n, n \\ 0 \leq t_j \leq T}} \left(\sum_{j=1}^n g_j P(t_j) - \gamma/2 \sum_{j,l=1}^n g_j g_l R(t_j - t_l) \right) \quad (3.25)$$

becomes

$$\max_{\substack{b_1, b_2, \dots, b_J \\ b_j \in B}} \sum_{j=1}^J b_j P(j\Delta) - \gamma/2 \sum_{j,l=1}^J b_j b_l R(j\Delta - l\Delta) \quad (3.26)$$

Here we note that maximization in (3.25) requires finding of maximizing $\{t_n^*\}$ and $\{g_n^*\}$ for each n and then choosing the maximum amongst these maxima. Such a complicated procedure is obviated in (3.26) by fixing J . We recognize the expression in (3.26) as the familiar likelihood function for

estimating b_m in presence of Gaussian noise when these are transmitted through a channel with impulse response $w(t)$. Thus b_m can be estimated using Viterbi algorithm as described by Forney [12]. Now the likelihood function can be written as

$$L_m(r(t)) \sim \exp(-\lambda_m) \prod_{j=1}^J [\lambda_m(j\Delta)]^{q_j} \quad (3.27)$$

Substituting $\lambda(t)$ from (2.2) in (3.27) we get

$$L_m(r(t)) \sim \exp\left(-\int_0^\tau \left(\sum_n a_n p(t-nT) + \lambda_o\right) dt\right).$$

$$\cdot \prod_{j=1}^J \left(\sum_n a_n p(j\Delta - nT) + \lambda_o\right)^{q_j} \quad (3.28)$$

Now the data sequence $\{a_n\}_{n=1}^N$ can be estimated by calculating the likelihood function (3.28) for all the possible 2^N sequences. Since $p(t)$ in (2.2) has finite duration, the likelihood function in (3.28) can be calculated recursively [10] and can be maximized using the Viterbi algorithm. Then the receiver structure is as shown in Fig. 3.1.

As we know that implementation of Viterbi-algorithm is quite complicated, in the next section, we derive a sub-optimum structure by assuming that past symbols are correctly known to the receiver. This gives rise to the decision feedback equalizer.



Fig. 3.1 FIBRE OPTIC RECEIVER

3.5 DECISION FEEDBACK EQUALIZER

The optimization of equation (3.26) can be done by Viterbi algorithm as pointed out earlier. We also know that a sub-optimum solution of this problem using decision feedback equalization exists. This is given by Austin [13] and Salz [14]. Hence we do not dwell upon optimization of (3.26) and assume that above receiver structures can be easily implemented. Now we go on to optimization of (3.28). Let us denote the impulse response $p(t)$ of the fibre as

$$p_1(t) = \begin{cases} p(t) & 0 \leq t < T \\ 0 & \text{otherwise} \end{cases} \quad (3.29)$$

$$p_2(t) = \begin{cases} p(t+T) & 0 \leq t < T \\ 0 & \text{otherwise} \end{cases}$$

$$\vdots$$

$$p_m(t) = \begin{cases} p(t+(m-1)T) & 0 \leq t < T \\ 0 & \text{otherwise} \end{cases}$$

where

$p(t)$ is non zero over the interval 0 to mT and zero for $t > mT$. When we are making decisions bit by bit then it is easy to note that if we are estimating the k th bit, our observation interval in (3.28) should be $(k-1)T$ to $(k+m-1)T$. Keeping this in mind we can write (3.28) as

$$L_m(r(t)) = \exp\left(-\sum_{n=k-m+1}^{k+m-1} a_n \int_{(k-1)T}^{(k+m-1)T} p(t-nT) dt + \lambda_0^m T\right).$$

$$\cdot \prod_{j=(k-1)J+1}^{kJ} \left(\sum_{n=k-m+1}^{k-1} a_n p_{k-n+1} (j\Delta - (k-1)J\Delta) + \right.$$

$$\left. a_k p_1 (j\Delta - (k-1)J\Delta) + \lambda_0 \right)^{q_j}$$

$$\cdot \prod_{j=kJ+1}^{(k+1)J} \left(\sum_{n=k-m+2}^{k-1} a_n p_{k-n+2} (j\Delta - kJ\Delta) + a_k p_2 (j\Delta - kJ\Delta) + \right.$$

$$\left. a_{k+1} (j\Delta - kJ\Delta) + \lambda_0 \right)^{q_j}$$

⋮

$$(k+m-1)J$$

$$\cdot \prod_{j=(k+m-2)+1}^{k+m-1} (a_k p_m (j\Delta - (k+m-2)J\Delta) +$$

$$\sum_{n=k+1}^{k+m-1} a_n p_{k+m-n} (j\Delta - (k+m-2)J\Delta) + \lambda_0)^{q_j} \quad (3.30)$$

Here we have split the terms in interval $(k-1)T$ to kT , kT to $(k+1)T$, ..., $(k+m-2)T$ to $(k+m-1)T$. At this point the natural thing to do would be to take the expectation of the likelihood function in (3.30), i.e., $L(r(t) | a_k, a_-) = E_{\{a_+\}} (L(r(t) | a_k, a_-, a_+))$. The likelihood function has the form, $\sum_n \exp(- \int \lambda_n(t) dt) \prod_{j=1}^{(m-1)J} [\lambda_m(j\Delta)]^{q_j}$. Here n takes 2^m values. Implementation of this likelihood function is difficult because we have to perform multiplications in 2^m channels and then add the results. Also in each channel the number of multiplications keep changing from interval to interval as the q_j 's which are non-zero keep changing in

each interval. This likelihood function is to be calculated for each hypothesis ($a_k = 0, a_k = 1$). But if we take the expectation of log-likelihood function with respect to future symbols, the receiver structure is greatly simplified. This gives a structure which is not optimum, but it is simpler to implement. Taking log of (3.30) and then averaging over equiprobable future symbols we get

$$\begin{aligned}
 L_A(r(t)) \Big|_{a_k, a^-} &= - \sum_{n=k-m+1}^{k-1} a_n p_{k+1-n} - a_k p_1 - \lambda_o^T \\
 &+ \sum_{j=1}^J q_{j+(k-1)J} \ln \left(\sum_{n=k-m+1}^k a_n p_{k+1-n} (j\Delta) + \lambda_o \right) \\
 &- \sum_{n=k-m+2}^{k-1} a_n p_{k+2-n} - a_k p_2 - \gamma_2 p_1 - \lambda_o^T \\
 &+ \gamma_2 \left(\sum_{j=1}^J q_{j+kJ} \ln \left(\sum_{n=k-m+2}^k a_n p_{k+2-n} (j\Delta) + \lambda_o \right) \right. \\
 &\quad \left. + \ln \left(\sum_{k-m+2}^k a_n p_{k+2-n} (j\Delta) + p_1 (j\Delta) + \lambda_o \right) \right) \\
 &- \sum_{n=k-m+r}^{k-1} a_n p_{k+r-n} - a_k p_r - \gamma_2 (p_1 + p_2 + \dots + p_{r-1}) - \lambda_o^T \\
 &+ \frac{1}{2^{r-1}} \sum_{j=1}^J q_{j+(k+r-2)J} \left[\sum_k \right. \\
 &\quad \left. \sum_{c_1, c_2, \dots, c_{r-1}} \ln \left(\sum_{n=k-m+r}^k p_{k+r-n} (j\Delta) + \lambda_o \right) + \right. \\
 &\quad \left. \sum_i c_i p_i (j\Delta) \right] \\
 &\vdots
 \end{aligned}$$

contd...

$$\begin{aligned}
 & -a_k p_m - \gamma/2(p_1 + p_2 + \dots + p_{m-1}) - \lambda_o^T \\
 & + \frac{1}{2^{m-1}} \sum_{j=1}^J q_{j+(k+m-2)J} \left(\sum_{\substack{c_1, c_2, \dots, c_{m-1} \\ c_i = (0, 1)}} \ln(a_m p_m(j\Delta)) + \right. \\
 & \quad \left. \lambda_o + \sum_i c_i p_i(j\Delta) \right) \tag{3.31}
 \end{aligned}$$

where we have used

$$\int_0^T P_j(t) dt = p_j \tag{3.32}$$

A zero or one is decided depending upon

$$L_A(r(t)|a_{k+1}, a^-) - L_A(r(t)|a_k=0, a^-) \geq 0 \tag{3.33}$$

Substituting (3.31) in (3.33) and cancelling out the common terms we get

$$\begin{aligned}
 & - \sum_{j=1}^m p_j + \sum_{j=1}^J q_{j+(k-1)J} \ln \left(1 + \frac{p_1(j\Delta)}{\sum_{n=k-m+1}^{k-1} a_n p_{k+1-n}(j\Delta) + \lambda_o} \right) \\
 & + \gamma/2 \sum_{j=1}^J q_{j+kJ} \ln \left(1 + \frac{p_2(j\Delta)}{\sum_{n=k-m+2}^{k-1} a_n p_{k+2-n}(j\Delta) + \lambda_o} \right) . \\
 & \cdot \left(1 + \frac{p_2(j\Delta)}{\sum_{n=k-m+2}^{k-1} a_n p_{k+2-n}(j\Delta) + p_1(j\Delta) + \lambda_o} \right) +
 \end{aligned}$$

$$+ \frac{1}{2^{r-1}} \sum_{j=1}^J q_{j+(k+r-2)J} \sum_{\substack{c_1, c_2, \dots, c_{r-1} \\ c_i = (0,1)}} .$$

$$\cdot \ln(1 + \frac{p_r(j\Delta)}{\sum_{n=k-m+r}^{k-1} a_n p_{k+r-n}(j\Delta) + \dots + \sum_i c_i p_i(j\Delta)})$$

+

•

•

•

$$+ \frac{1}{2^{m-1}} \sum_{j=1}^J q_{j+(k+m-2)J} \sum_{\substack{c_1, c_2, \dots, c_{m-1} \\ c_i = (0,1)}} \ln(1 + \frac{p_m(j\Delta)}{\lambda_0 + \sum_i c_i p_i(j\Delta)})$$

(3.34)

The receiver so obtained is shown in Fig. 3.2. In the next section we discuss some of the hardware features and complexity of the receiver.

3.6 RECEIVER COMPLEXITY

The receiver shown in Fig. 3.2, requires a memory of size $2^{m-1} \times J \times m$ where m is the number of bauds for which impulse response $p(t)$ is non-zero, J is no. of samples per baud ($J = T/\Delta$). Since we are required to store values $\ln(1+p_i(j\Delta))$ in the memory, we give some estimate of word size. For the impulse response considered (shown in Fig. 2.2) the maximum value is $\ln(1+37.3) = 3.7$ and the minimum value is $\ln(1+2.1 \times 10^{-3}) = 2.1 \times 10^{-3}$. For this range of numbers we require 12-bit words. The $(m-1)$ serial shift registers

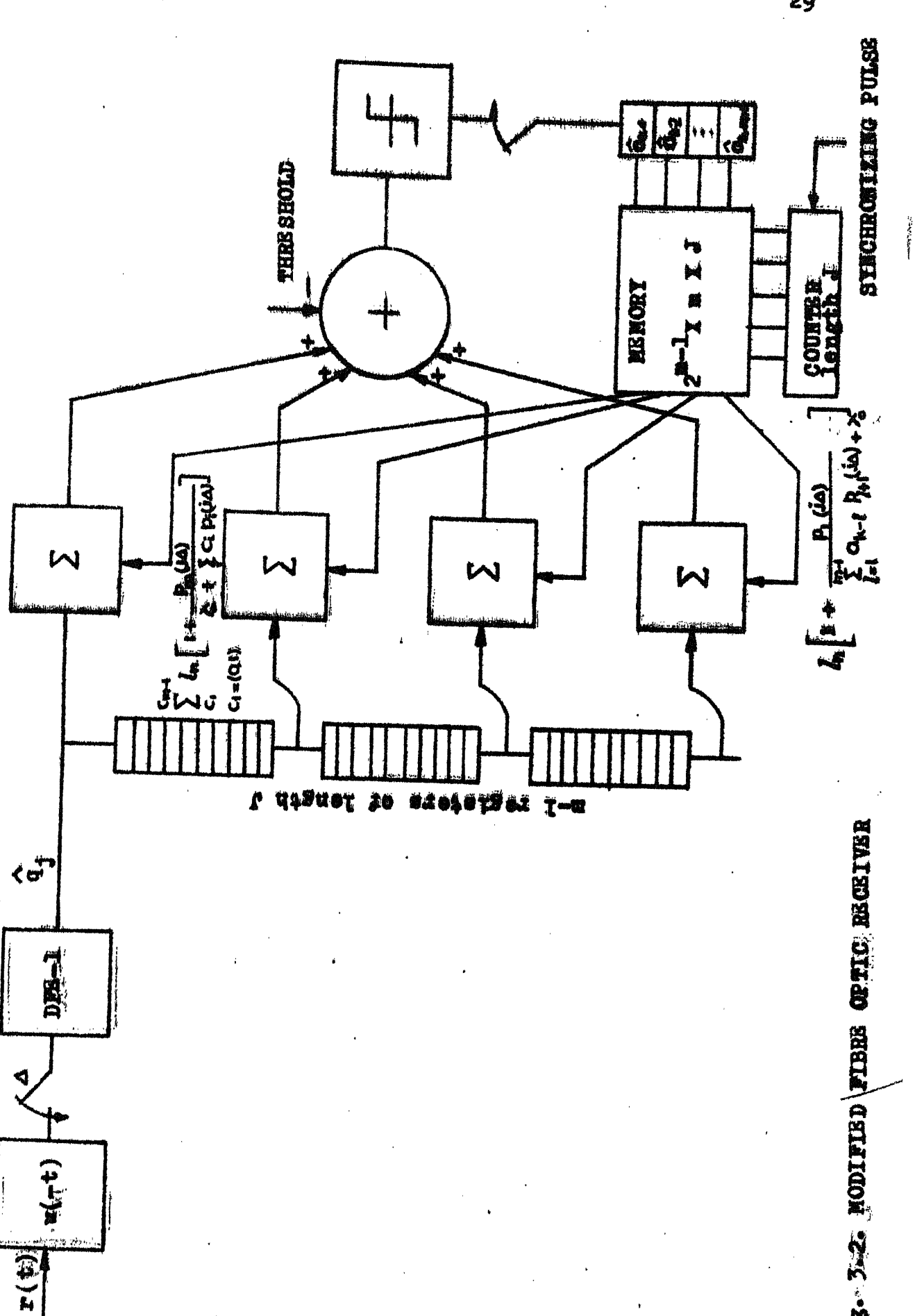


Fig. 3.2. MODIFIED FIBRE OPTIC RECEIVER

required to store q_j 's should be J bits long each. Then we require m -summers and m -accumulator registers. Since average number of photons received is 100 to 200, the threshold will be around these numbers. Hence accumulator register should be 17-bits long. We will show in the next chapter the number of samples required per baud is approximately twice the number of average electrons, hence, J will range from 200 to 400.

CHAPTER 4

PERFORMANCE OF THE DECISION FEEDBACK EQUALIZER

In this chapter we evaluate the performance of the Decision Feedback Equalizer obtained in the last chapter. Also, we compare its performance with an 'Integrate and Dump' receiver, 'One Band' receiver and 'Ideal' receiver. Numerical calculation of the probability of error calls for a great deal of computer time (approx. 30 min.). To overcome this difficulty, we calculate an upper bound on the probability of error. The upper bound on the probability of error is obtained by considering the situation in which intersymbol interference effects are the worst that can occur.

The intersymbol interference may aid or hinder the detection of a symbol depending upon whether the symbol is '1' or '0'. When we are trying to detect a symbol '1' in the presence of ISI, and the symbols preceding and following it are all '1', then these will help in detection by producing more electrons. But if we are detecting a symbol '0' in the above situation, the probability of error will be large. Similarly, detection of a '1' in the midst of all zero's will have a probability of error larger than that for any other combination of the preceding and following symbols. Hence two worst conditions

JAWAHARLAL NEHRU TECHNOLOGICAL UNIVERSITY
CENTRAL LIBRARY

Acc. No. A 66893

detection of a '1' in all zero's, and detection of a zero in all one's. These give the upper bound on the probability of error. In calculating these probabilities, we fixed the threshold such that the probability of error was same in both of these worst cases.

Closed form expressions for the probability of error in the above cases are not available. The probability of error can be evaluated only by numerical methods. One such method suitable for our purpose is Gram-Charlier series expansion method [15-17]. We will describe this method in the next section.

We have also compared our analytical results with simulation studies. Since large computer time (approx 30 min) is required, we simulated the receiver only for the case when $\lambda = 50$ (= average number of electrons emitted by a single pulse).

4.1 GRAM-CHARLIER SERIES EXPANSION METHOD

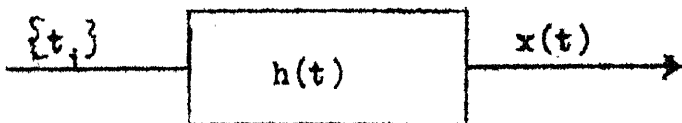


Fig. 4.1

Let $\{t_i\}$ be a series of impulses whose arrival times are Poisson distributed with the mean intensity $\lambda(t)$. The moment generating function of the random variable $x(t)$ is

$$M_x(s) = E(\exp(sx(t)))$$

$$= E(\exp(s \sum_{j=1}^{k(t)} h(t-t_j))) \quad (4.1)$$

where $k(t)$ is the number of counts in the interval $(0, t)$ and $\{t_j\}$ are arrival instants. To calculate this expectation, first we find the conditional expectation conditioned on the number of counts, and then average over the number of counts, i.e.,

$$\begin{aligned} M_x(s) &= E_k \left[E_t \left(\exp \left(s \sum_{j=1}^{k(t)} h(t-t_j) \right) | k \right) \right] \quad (4.2) \\ &= E_k \left[\int_0^t \int_0^t \cdots \int_0^t \exp \left(s \sum_{j=1}^{k(t)} h(t-t_j) \right) p(t_1, t_2, \dots, t_k | k) \right. \\ &\quad \left. dt_1 dt_2 \cdots dt_k \right] \\ &= E_k \left(\prod_{j=1}^k \int_0^t \exp(s h(t-t_j)) \frac{\lambda(t_j)}{\Lambda} dt_j \right) \\ &= E_k [(M_n(s))^k] \end{aligned}$$

where

$$M_n(s) = \int_0^t \exp(s h(t-z)) \frac{\lambda(z)}{\Lambda} dz \quad (4.3)$$

Averaging over k yields :

$$\begin{aligned} M_x(s) &= \sum_{k=0}^{\infty} \frac{\Lambda}{k!} e^{-\Lambda} M_n^k(s) \quad (4.4) \\ &= \exp[(M_n(s)-1)\Lambda] \\ &= \exp \left[\int_0^t (\exp(sh(t-z)) \lambda(z) - \lambda(z)) dz \right] \end{aligned}$$

Expanding the inner exponential term by Taylor series, we get :

$$M_x(s) = \exp\left(\sum_{q=1}^{\infty} \frac{s^q}{q!} \int_0^t h^q(t-z) \lambda(z) dz\right) \quad (4.5)$$

Therefore, this has cummulants (semi-invariants) as

$$\gamma_q = \int_0^t h^q(t-z) \lambda(z) dz \quad (4.6)$$

Since the numerical values of these cummulants increase with q , we consider the normalized process

$$\hat{x}(t) = \frac{x(t) - \gamma_1}{\sqrt{\gamma_2}} \quad (4.7)$$

This has moment generating function as

$$\begin{aligned} M_{\hat{x}}(s) &= E[\exp(s\hat{x})] \\ &= M_x\left(\frac{s}{\sqrt{\gamma_2}}\right) \exp\left(-\frac{s\gamma_1}{\sqrt{\gamma_2}}\right) \\ &= \exp\left(\sum_{q=1}^{\infty} \frac{s^q}{q!} \frac{1}{\gamma_2^{q/2}} \gamma_q - \frac{s\gamma_1}{\sqrt{\gamma_2}}\right) \\ &= \exp\left(\sum_{q=1}^{\infty} \frac{s^q}{q!} \hat{\gamma}_q\right) \end{aligned} \quad (4.8)$$

where

$$\begin{aligned}\hat{\gamma}_1 &= 0 \\ \hat{\gamma}_2 &= 1 \\ \hat{\gamma}_q &= \frac{\gamma_q}{\gamma_2^{q/2}}, \quad q > 2\end{aligned}\tag{4.9}$$

One way to obtain the density function of a random variable from knowledge of its cumulants is to use the Gram-Charlier series expansion of the density function, namely

$$p(x) = \sum_{n=0}^{\infty} c_n H_n(x)\tag{4.10}$$

where

$$H_n(x) = \frac{d^n}{dx^n} \left[\frac{1}{\sqrt{2\pi}} \exp(-x^2/2) \right]\tag{4.11}$$

The corresponding moment generating function of $p(x)$ is

$$\begin{aligned}M_x(s) &= \int_{-\infty}^{\infty} \exp(sx) p(x) dx \\ &= \sum_{n=0}^{\infty} c_n \int_{-\infty}^{\infty} \exp(sx) \frac{d^n}{dx^n} \frac{1}{\sqrt{2\pi}} \exp(-x^2/2) dx \\ &= \sum_{n=0}^{\infty} c_n (-1)^n s^n \exp(s^2/2) \\ &= \sum_{n=0}^{\infty} \mu_n \frac{s^n}{n!} \exp(s^2/2)\end{aligned}\tag{4.12}$$

where

$$\mu_n = (-1)^n c_n n!\tag{4.13}$$

The coefficients, C_n , in the expansion (4.10) can be calculated from knowledge of cumulants, by equating the moment generating function calculated in (4.8) and (4.12).

$$\exp\left(\frac{s^2}{2} + \sum_{n=3}^{\infty} \hat{\gamma}_n \frac{s^n}{n!}\right) = \exp(s^2/2) \sum_{n=0}^{\infty} \frac{\mu_n}{n!} s^n \quad (4.14)$$

Expanding the left-hand side expression, after cancelling the common factor $\exp(s^2/2)$, we get

$$\begin{aligned} \exp\left(\sum_{n=3}^{\infty} \hat{\gamma}_n \frac{s^n}{n!}\right) &= 1 + \sum_{n=3}^{\infty} \hat{\gamma}_n \frac{s^n}{n!} + \frac{1}{2} \left(\sum_{n=3}^{\infty} \hat{\gamma}_n \frac{s^n}{n!}\right)^2 + \dots \\ &\quad + \frac{1}{r!} \left(\sum_{n=3}^{\infty} \hat{\gamma}_n \frac{s^n}{n!}\right)^r + \dots \quad (4.15) \\ &= 1 + \hat{\gamma}_3 \frac{s^3}{3!} + \hat{\gamma}_4 \frac{s^4}{4!} + \hat{\gamma}_5 \frac{s^5}{5!} + (\hat{\gamma}_6 + \hat{\gamma}_3 \frac{6!}{(3!)^2}) \frac{s^6}{6!} + \dots \end{aligned}$$

Equating coefficients of both sides of (4.14) using (4.15) we get

$$\mu_0 = 1 \quad (4.16)$$

$$\mu_1 = 0$$

$$\mu_2 = 0$$

$$\mu_3 = \hat{\gamma}_3$$

$$\mu_{n+1} = \hat{\gamma}_{n+1} + \sum_{m=2}^{n-1} \hat{\gamma}_{m+1} \mu_{n-m}; \quad n \geq 3$$

The coefficients, C_n , can be calculated using equation (4.13).

The functions, $H_n(x)$, can also be calculated recursively by noting that

$$H_n(x) = -(xH_{n-1}(x) + (n-1)H_{n-2}(x)); n \geq 2 \quad (4.17)$$

where

$$H_0(x) = \frac{1}{\sqrt{2\pi}} \exp(-x^2/2).$$

and

$$H_1(x) = -\frac{x}{\sqrt{2\pi}} \exp(-x^2/2)$$

The probability of error can be calculated using the following two relations

$$\begin{aligned} \int_{-\infty}^{x_0} p(x)dx &= \int_{-\infty}^{x_0} \sum_{n=0}^{\infty} C_n H_n(x)dx \\ &= \int_{-\infty}^{x_0} H_0(x)dx + \sum_{n=3}^{\infty} C_n \int_{-\infty}^{x_0} H_n(x)dx \\ &= \int_{-\infty}^{x_0} \frac{1}{\sqrt{2\pi}} \exp(-x^2/2)dx + \sum_{n=3}^{\infty} C_n \int_{-\infty}^{x_0} \frac{d}{dx} H_{n-1}(x)dx \\ &= \frac{1}{2} \operatorname{erfc}(-x_0) + \sum_{n=3}^{\infty} C_n H_{n-1}(x_0); x_0 < 0 \end{aligned} \quad (4.18)$$

$$\text{where } \operatorname{erfc}(y) = 1 - \int_0^y \frac{2}{\sqrt{\pi}} \exp(-x^2/2)dx \quad (4.19)$$

Similarly, we have

$$\int_{x_0}^{\infty} p(x)dx = \frac{1}{2} \operatorname{erfc}(x_0) - \sum_{n=3}^{\infty} C_n H_{n-1}(x_0); x_0 > 0 \quad (4.20)$$

The equalizer we derived in the last chapter (fig.3.2) operates on \hat{q}_j 's, the estimates of arrival times. But some of these estimates will be incorrect because of the thermal noise in the first detector. So we can write the output of first detector as

$$\hat{q}_j = q_j + p_j \quad (4.21)$$

where $p_j = \pm 1, 0$. $p_j = 1$ means we detect an electron emission when in fact there is none.

Similarly, $p_j = -1$ means we fail to detect an emitted electron. $p_j = 0$ means no error. To take into account this situation, we assume that input to filter, $h(t)$, in Fig. 4.1 is

$$\sum_{j=0}^{k(t)} \delta(t-t_j) + \sum_{j=0}^{k_e(t)} e_j \delta(t-z_j) \quad (4.22)$$

The first term is the same as in the previous discussion.

The second term takes into account the errors. $e_j = \pm 1$, $\{z_j\}$ is arrival time of those error impulses, and $k_e(t)$ is the number of errors in the interval 0 to t .

We now make some simplifying assumptions about the statistics of the error process. We assume that

- (1) $\{e_j\}$ are independent of each other and $e_j = \pm 1$ are equiprobable.

(2) The arrival time Z_j is uniform in time interval $0-T$.
 (3) The error process $\{Z_j\}$ is independent of the process $\{t_j\}$.

The assumptions (1) and (2) are not quite correct because the errors in the first DFE will actually be in bursts. But for simplicity we assume the errors to be random. Then, by assumption (1), the number of errors in time T will obey binomial distribution, which can be approximated by a Poisson distribution. Hence we make the fourth assumption that

(4) The number of errors, $k_e(T)$, in time interval of T is Poisson with mean e .

Now the output of the filter $h(t)$ due to the error process $\{Z_j\}$ will be

$$E(T) = \sum_{j=0}^{k_e(T)} e_j h(T-Z_j) \quad (4.23)$$

Proceeding as before, we can write the moment generating function of the output error process as

$$\begin{aligned} M_{\bar{e}}(s) &= E \left[\exp(s E(T)) \right] \quad (4.24) \\ &= E_k, \{e_j\} \left[\prod_{j=1}^k \int_0^T \exp(se_j h(T-z)) \frac{1}{T} dz \right] \end{aligned}$$

Since $e_j = \pm 1$ are equiprobable we get

$$M_E(s) = E_k \left[\frac{1}{2^k} \sum_{r=0}^k \binom{k}{r} A^r B^{k-r} \right] \quad (4.25)$$

where

$$A = \int_0^T \frac{1}{T} \exp(sh(T-z)) dz \quad (4.26)$$

and

$$B = \int_0^T \frac{1}{T} \exp(-s h(T-z)) dz$$

Simplifying (4.25) we get

$$M_E(s) = E_k \left[\left(\frac{A+B}{2} \right)^k \right] \quad (4.27)$$

$$= \sum_{k=0}^{\infty} \frac{e^k}{k!} \exp(-e) \left(\frac{A+B}{2} \right)^k$$

$$= \exp \left[\left(\frac{A+B}{2} - 1 \right) e \right]$$

$$= \exp \left[\int_0^T \frac{e}{2T} \exp(sh(T-z)) dz + \int_0^T \frac{e}{2T} \exp(-sh(T-z)) dz - e \right]$$

Expanding the inner exponential term, we get

$$\begin{aligned} M_E(s) &= \exp \left[\frac{e}{2} \sum_{q=1}^{\infty} \frac{s^q}{q!} \int_0^T h^q(T-z) \frac{1}{T} dz + \frac{e}{2} \sum_{q=1}^{\infty} \frac{(-1)^q s^q}{q!} \int_0^T h^q(t-z) dz \right] \\ &= \exp \sum_{q=2, \text{ even}}^{\infty} \frac{s^q}{q!} \beta_q \end{aligned} \quad (4.28)$$

where

$$\beta_q = \int_0^T (e/T) h^q(T-z) dz ; q \text{ even} \quad (4.29)$$

Since the processes $\{t_j\}$ and $\{z_j\}$ are independent, the moment generating function of the output process will be obtained by multiplying (4.28) and (4.5).

$$M_y(s) = M_x(s) \cdot M_E(s)$$

$$= \exp\left(\sum_{q=1}^{\infty} \frac{s^q}{q!} \gamma_q + \sum_{q=2, \text{even}}^{\infty} \frac{s^q}{q!} \beta_q\right) \quad (4.30)$$

The expressions (4.7) to (4.16) are still valid if we replace γ_q by $(\gamma_q + \beta_q)$, where it is understood that $\beta_q = 0$ for q odd. Hence, we can calculate the probability of error using (4.18) and (4.20).

4.2 NUMERICAL RESULTS

In the previous section we outlined a procedure to calculate the probability of error. In this section we use this procedure to calculate an upper-bound on the probability of error by calculating the PE for worst case of ISI. We compare the performance of the decision feedback equalizer with several other receiver structures. These receiver structures are

- (1) Integrator and Dump : Here the filter $h(t)$ has the response $h(t) = 1; 0 \leq t < T$, and $h(t) = 0$ otherwise. This is the simplest receiver and in fact, is nothing more than a counter.

(2) One Baud receiver : This is also a decision feedback equalizer. But here we decide about the symbol after the first baud only. Therefore, there is no future symbol interference. But there is a loss of signal energy as the energy in the first baud only is being utilized.

(3) Ideal : In this receiver we assume that only the symbol being detected is unknown to the receiver, all other symbols, past or future are known to the receiver.

For the purpose of calculations we have used the impulse response of fibre as shown in Fig. 2.2 with $Z = 10$ km. The time interval T is taken to be 150 ns. When an average of 50 primary electrons are emitted by the photo-detector, then the number of electrons in the first and second baud are 27.7 and 20.1, respectively. We assume that the response extends upto three bauds only. The upper bound is calculated by calculating the error probability for the sequence 00100. The coefficients, c_n of the Gram-Charlier series were obtained by eqns. (4.6), (4.9), (4.13) and (4.16). For calculating the cummulants γ_q 's the appropriate impulse responses $h(t)$ were taken. These impulse responses are :

For 'Integrate and Dump' receiver

$$h(T-t) = \begin{cases} 1 & 0 \leq t < T \\ 0 & \text{otherwise.} \end{cases} \quad (4.31)$$

For 'One Baud' receiver

$$h(kT-t) = \ln\left(1 + \frac{p_1(t)}{a_{k-2}p_3(t) + a_{k-1}p_2(t) + \lambda_0}\right); (k-1)T \leq t < kT \quad (4.32)$$

For 'Decision Feedback Equalizer'

$$\begin{aligned} h((k+2)T-t) &= \ln\left(1 + \frac{p_1(t)}{a_{k-2}p_3(t) + a_{k-1}p_2(t) + \lambda_0}\right); (k-1)T \leq t < kT \\ &= \frac{1}{2} \ln\left(1 + \frac{p_2(t)}{a_{k-1}p_3(t) + \lambda_0}\right)\left(1 + \frac{p_2(t)}{a_{k-1}p_3(t) + p_1(t) + \lambda_0}\right); \\ &\quad kT \leq t < (k+1)T \\ &= \frac{1}{4} \ln\left(1 + \frac{p_3(t)}{\lambda_0}\right)\left(1 + \frac{p_3(t)}{\lambda_0 + p_1(t)}\right)\left(1 + \frac{p_3(t)}{\lambda_0 + p_2(t)}\right) \\ &\quad \left(1 + \frac{p_3(t)}{\lambda_0 + p_1(t) + p_2(t)}\right); (k+1)T \leq t < (k+2)T \end{aligned}$$

For 'Ideal' Receiver

$$\begin{aligned} h((k+2)T-t) &= \ln\left(1 + \frac{p_1(t)}{a_{k-2}p_3(t) + a_{k-1}p_2(t) + \lambda_0}\right); (k-1)T \leq t < kT \\ &= \ln\left(1 + \frac{p_2(t)}{a_{k-1}p_3(t) + \lambda_0 + a_{k+1}p_1(t)}\right); (kT) \leq t < (k+1)T \\ &= \ln\left(1 + \frac{p_3(t)}{\lambda_0 + a_{k+1}p_2(t) + a_{k+2}p_1(t)}\right); (k+1)T \leq t < (k+2)T \quad (4.33) \end{aligned}$$

The probability of error was calculated using eqns. (4.18) to (4.20).

Table 4.1 shows the probability of error for different types of receiver when there is no error in the estimates of arrival time of photons. The probability of error is plotted in Fig. 4.2. In Tables 4.2 and 4.3 the probability of error is calculated when the average number of errors in the estimates of

Table 4.1

Probability of error when $e = 0$

Number of primary electron Λ	Integrate and Dump P_e	One Baud P_e	DFE	Ideal P_e
50	.8456421E-02	.4092009E-03	.4060567E-04	.3300548E-05
100	.3931534E-03	.9398552E-06	.2053243E-07	.6598730E-10
150	.2467062E-04	.2347858E-08	.4504045E-10	.3838555E-13
200	.1108633E-05	.8101825E-11	.1496475E-12	.1117890E-15
250	.8428228E-07	.6615635E-13	.3731193E-15	.2136018E-18
300	.5082812E-08	.8943073E-15	.2350956E-17	.5437326E-21
350	.3110747E-09	.3705406E-16	.8862890E-19	.8507042E-24
400	.6547161E-11	.9203830E-18	.2328687E-21	.1183835E-26

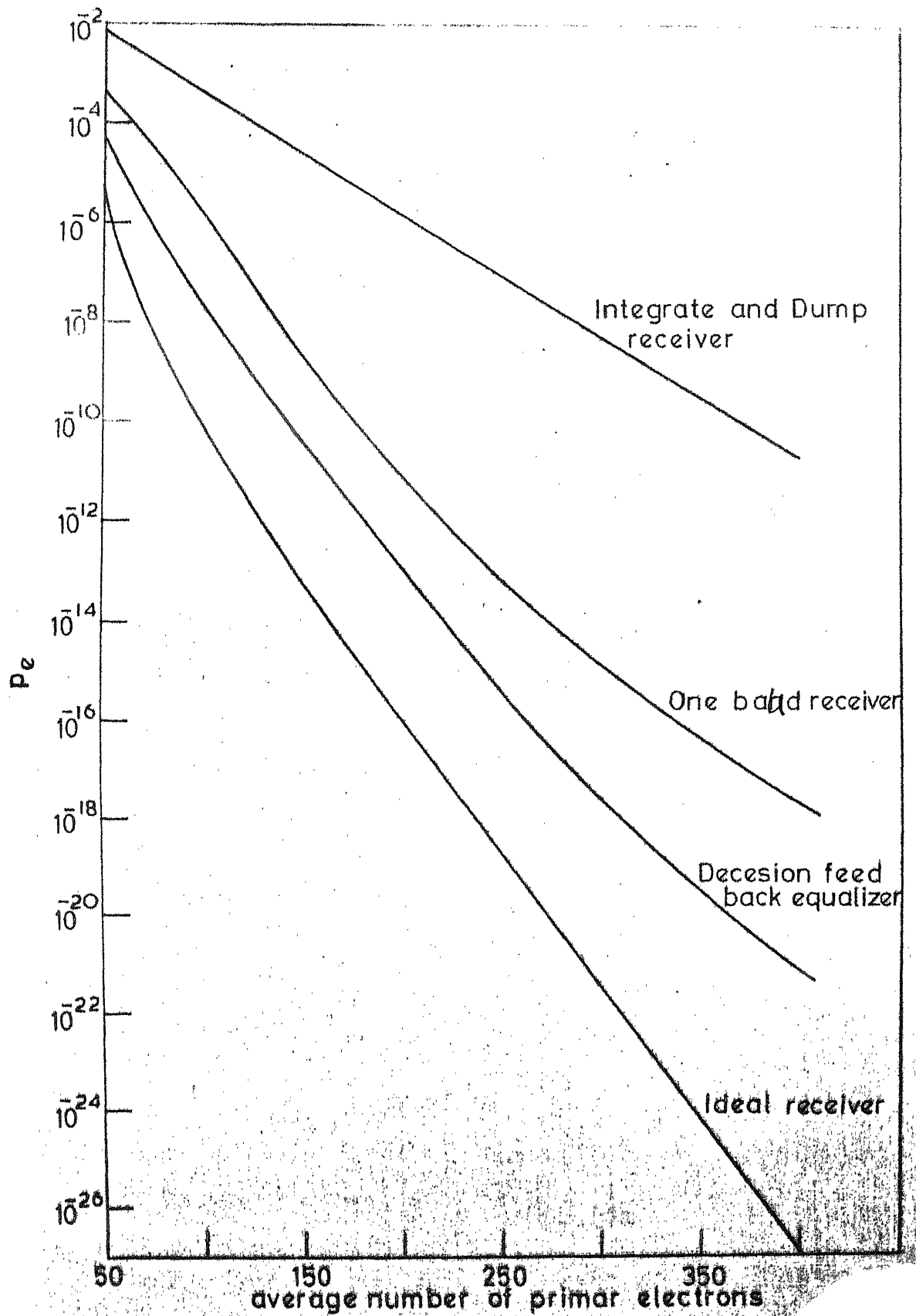


FIG. 4.2 PROBABILITY OF ERROR WHEN $\epsilon/\Lambda = 0$

arrival time is 2%, and 5%, of the average number of photons received. The results are plotted in Figs. 4.3 and 4.4.

From the plots in Fig. 4.2, 4.3 and 4.4, we can conclude that DFE is 3.5 dB better than as Simple Integrate and Dump receiver. It is better than a One Baud receiver by 0.82 dB. But the DFE is inferior to Ideal receive by 1.4 dB. These calculations are for the case when the probability of error is 10^{-13} .

To see the effect of errors in the estimation of arrival time, we have calculated the probability of error for different values of e/λ (e = average number of errors in one baud). The results are tabulated in Table 4.4 and shown as a graph in Fig. 4.5. From these we see that the system degradation is not very large.

4.3 SIMULATION RESULTS

The DFE in Fig. 3.2 was simulated for average number of primary electrons equal to 50. First, we simulated the receiver when the input sequence was 00100. The feedback filter contained 00 and the feedback path was broken. This corresponds to the model used in the previous section to calculate the upper bound on PE. A computer-run with 10^4 iterations gave 2-errors. Another run with 10^5 iterations gave 18 errors. This gives the PE as 2×10^{-4} , 5 times more than the value calculated in the previous section. The time taken for 10^5 iterations was approximately 30 min so we did not make further trials.

Table 4.2

Probability of error when $(e/\eta) = 10^2$

No. of primary electron λ	Integrate and Dump P_e	One baud receiver P_e	DIF P_e	Ideal P_e
50	.1112345E-01	.6583533E-03	.8017150E-04	.9086089E-05
100	.65543416E-03	.2453981E-05	.4167411E-07	.5708442E-09
150	.4284386E-04	.1019593E-07	.1025356E-09	.5692077E-12
200	.2946548E-05	.4256048E-10	.6675696E-12	.1037558E-14
250	.2066524E-06	.3132443E-12	.1957957E-14	.3356593E-17
300	.1481057E-07	.4130461E-14	.1298044E-16	.4456507E-20
350	.1075712E-08	.6263903E-15	.1673259E-18	.9450486E-23
400	.4965956E-10	.4890014E-17	.1224541E-20	.2179891E-25

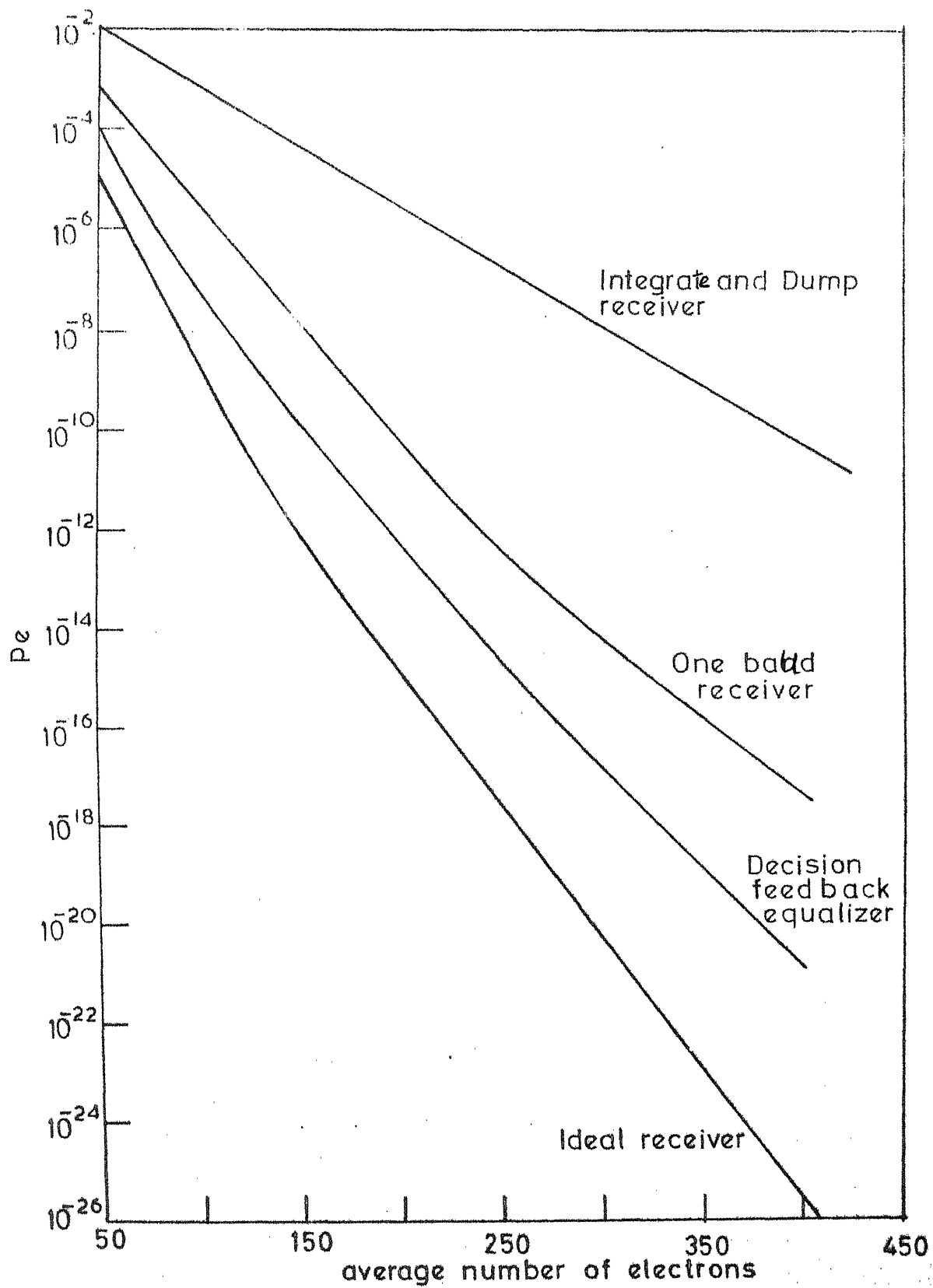


FIG. 4.3 PROBABILITY OF ERROR WHEN $e/\Lambda = .02$

Table 4.3

Probability of error when $(e/\kappa) = 0.5$

No. of primary electrons κ	Integrate & Dump P_e	One Baud receiver P_e	DFE P_e	Ideal P_e
50	.1454193E-01	.1154682E-02	.1775520E-3	.2801344E-04
100	.1074902E-02	.7488463E-05	.2024430E-6	.5334061E-08
150	.8804801E-04	.5415556E-07	.4180395E-9	.4179037E-11
200	.7553665E-05	.4139589E-09	.2008073E-11	.9037558E-14
250	.6656398E-06	.3144585E-11	.9044495E-14	.2573935E-16
300	.5968472E-07	.3207197E-13	.8265503E-16	.6569859E-19
350	.5418894E-08	.9867540E-15	.7531707E-18	.1532051E-21
400	.7870329E-10	.3191646E-16	.7289399E-20	.3967191E-24

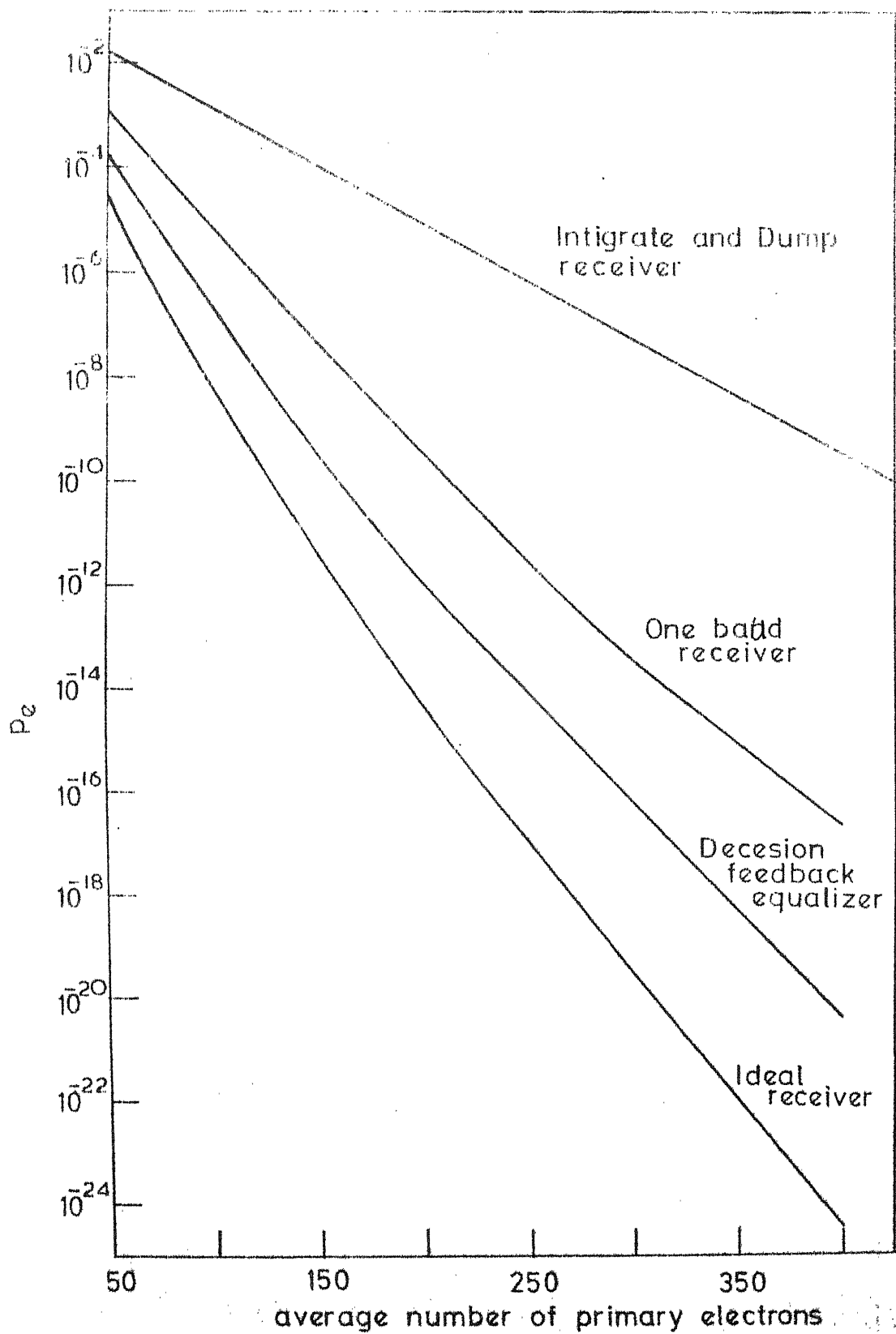


FIG.4.4 PROBABILITY OF ERROR WHEN $e/\Lambda = 0.05$

Table 4.4

Variation of probability of error with e/λ

λ	$e/\lambda = 0$	$e/\lambda = .01$	$e/\lambda = .02$	$e/\lambda = .03$	$e/\lambda = .04$	$e/\lambda = .05$
100	.2053243E-07	.3106612E-07	.4167411E-07	.1204142E-06	0.1620486E-06	.2024430E-6
200	.1496475E-12	.2646541E-12	.6675696E-12	.1431773E-11	0.1891205E-11	.2008073E-11

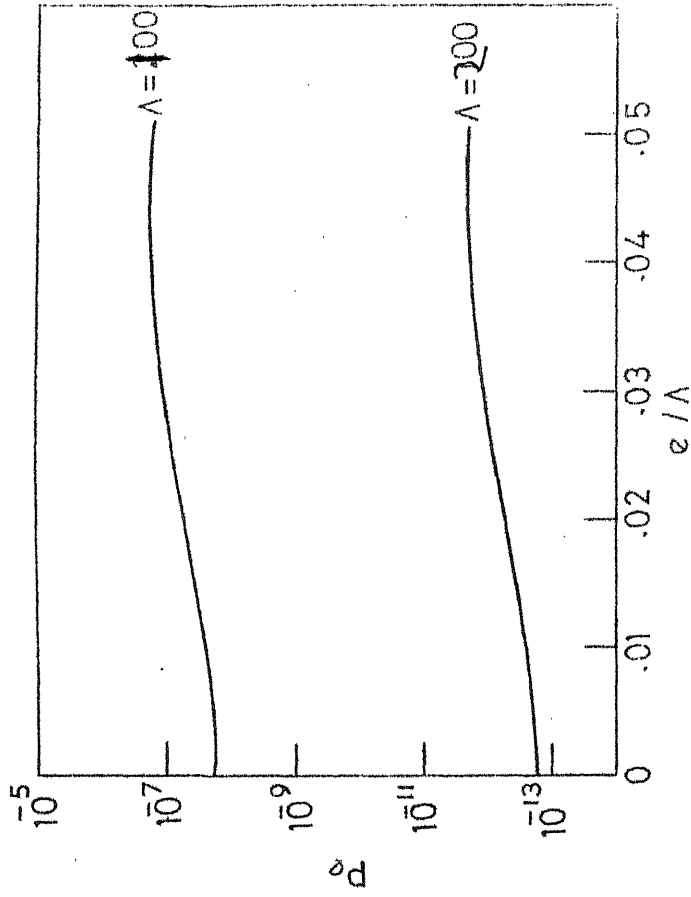


FIG. 4.5 VARIATION OF PROBABILITY OF ERROR WITH ERRORS IN ELECTRON ARRIVAL ESTIMATES

The simulation of actual DFE, when input symbols were also random, gave 21 errors in 10^5 iterations. This number is approximately same as above, indicating that there was no error propagation in the DFE.

We also simulated the One Baud receiver. Computer-runs of 10^4 iterations gave number of errors at 9, 8 and 11 in three different trials. This is equivalent to $PE = 10^{-3}$, which is 2.5 times the PE calculated numerically in the last section. The reason for discrepancy may be that we took the arrival times in the previous section to be continuous while here we are quantizing the arrival times.

4.4 TIMING ERROR EFFECTS

In calculating the probability of error, we have been assuming that the bit timing is perfect and the decoder is perfectly synchronized. If timing offsets occur during a bit period, because of inaccurate time synchronization of the transmitter and receiver, processing takes place in offset intervals, leading to system degradation. To get an idea of this, we assume that the sequence 00100 is repeated. Then we calculate the probability of error for various $\Delta T/T$ timing offset values. The results are tabulated in Table 4.5 and plotted in Fig. 4.6. The results show a large degradation (increase in probability of error) as the timing offset reaches .5. The timing offsets effectively decrease the signal energy and increase the noise.

Table 4.5

Effect of time shift

$\Delta T/T$	$\lambda = 100$ P_e	$\lambda = 200$ P_e
0	0.2024430E-06	0.2008073E-11
.1	0.1435179E-05	0.1642984E-10
.2	0.1643697E-04	0.1997740E-08
.3	0.1689365E-03	0.1891100E-06
.4	0.1019190E-02	0.6147204E-05
.5	0.2832715E-02	0.4366327E-04
.6	0.3394822E-02	0.6187912E-04
.7	0.1700239E-02	0.1643831E-04
.8	0.3151896E-03	0.6328524E-06
.9	0.1684392E-04	0.2089586E-08

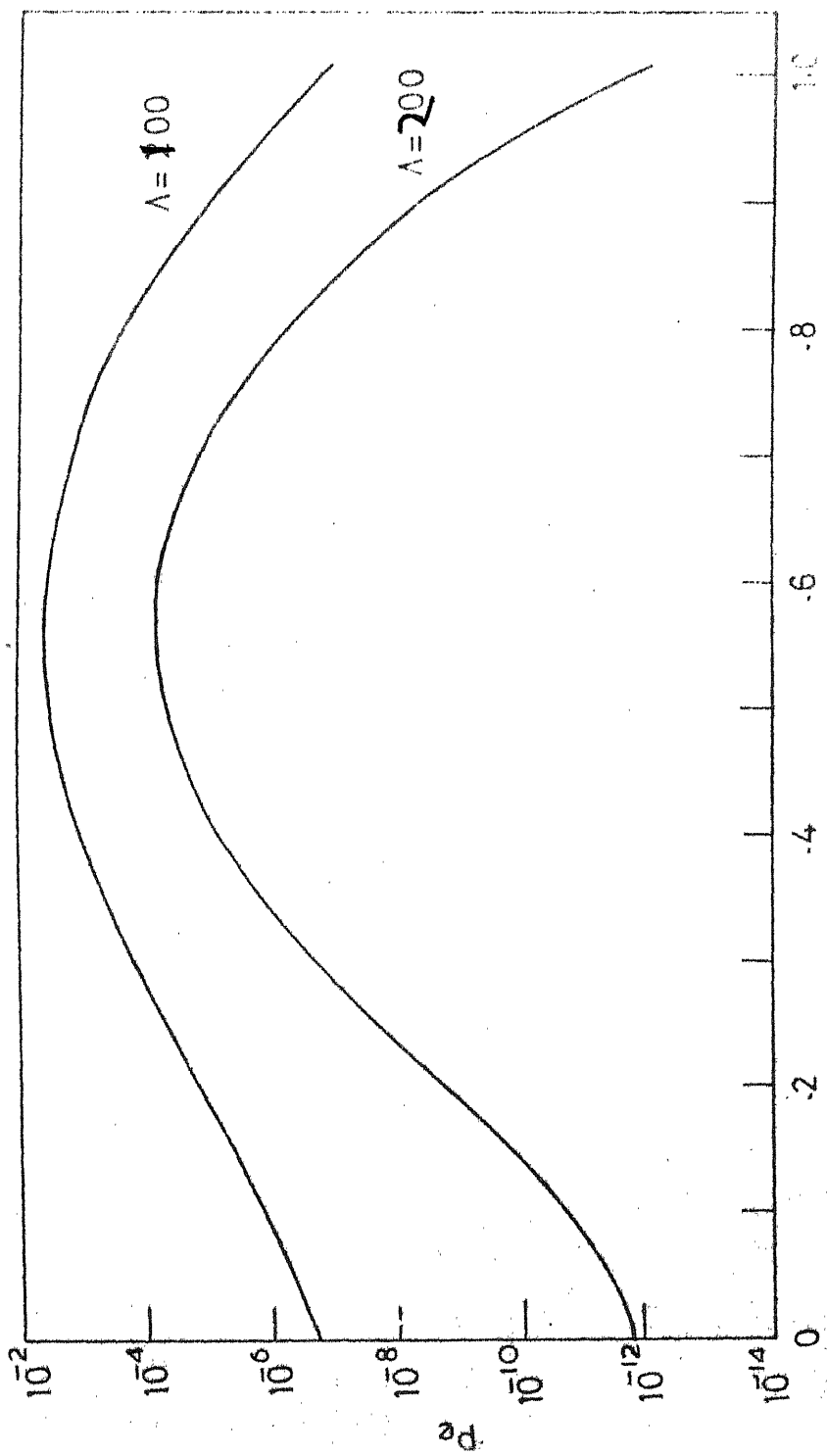


FIG. 4.6 VARIATION OF PROBABILITY OF ERROR WITH TIME STEP ERROR
 ΔT

4.5 EFFECT OF SAMPLING RATE

The number of electrons emitted, n , by the photodetector is a random number, Poisson distributed with mean λ (average number of electrons due to one pulse). Since we are taking only $J (= T/\Delta)$ samples per baud, we will not be able to detect all the emitted electrons. The probability that the number of emitted electrons, n is greater than J , is given by

$$P(n > J) = \sum_{k=J+1}^{\infty} \frac{\exp(-\lambda)}{k!} \lambda^k \quad (4.34)$$

This probability can be evaluated in terms of incomplete gamma function [1]

$$\Gamma(n, x) = \int_0^x \exp(-t) t^{n-1} dt \quad (4.35)$$

by using the identity

$$\sum_{k=J+1}^{\infty} \frac{\exp(-\lambda)}{k!} \lambda^k = \frac{\Gamma(J+1, \lambda)}{\Gamma(J+1, \infty)} \quad (4.36)$$

These values are tabulated in Table 4.6 for $\lambda = 50$ and $\lambda = 100$. Also, we have tabulated the average number of electrons that can be detected in one baud. These values are obtained by generating a Poisson random variable in the digital computer and then counting the electrons detected in a baud interval. The results are plotted in Fig. 4.7. We see that if $J = 2\lambda$, the average number of electrons detected is approximately λ , also the probability that n is greater than 2λ is very small. So a sampling

Table 4.6

Variation in average number of Electrons emitted with sampling rate J

Sampling rate J	Average No. of detected electron n $\wedge = 50$	Prob(n > J) \wedge	Average No. of detected electron n $\wedge = 100$	Prob (n > J) $\wedge = 100$
50	36.39	.546		
60	39.44	.104		
70	41.87	.534E-2		
80	43.88	.762E-4		
90	46.98	.335E-6		
100	48.14	.509E-9	72.38	.145
110	48.74	.291E-12	75.59	.107
120	50.54	.686E-16	79.38	.120E-2
130	51.03	.710E-20	81.90	.345E-4
140	50.95	.333E-24	84.13	.478E-6
150	51.23	.818E-29	86.87	.333E-8
160			88.22	.121E-10
170			90.66	.242E-13
180			93.04	.270E-16
190			94.16	.174E-19
200			96.74	.619E-23

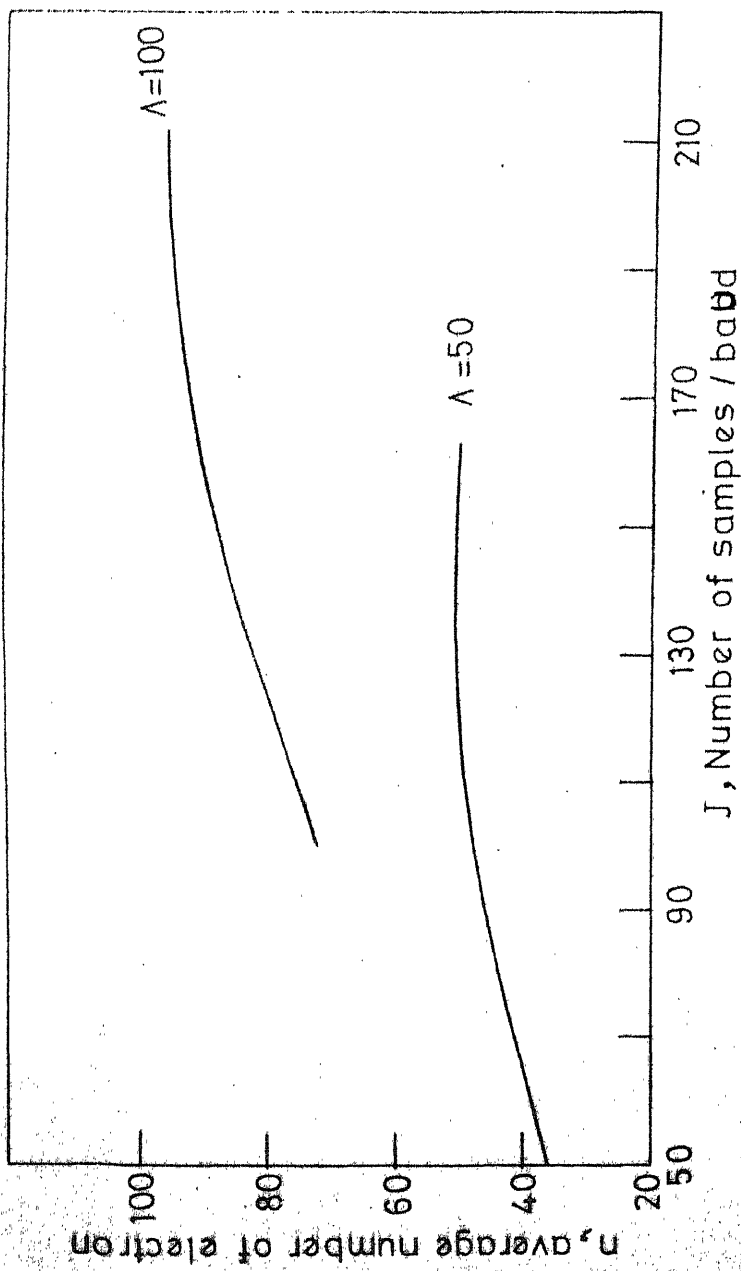


FIG. 4-7 VARIATION IN NUMBER OF ELECTRONS DETECTED WITH CHANGE IN NUMBER OF SAMPLES J PER BAND

frequency which is twice the number of average electrons emitted is sufficient. Moreover, it will not be required to detect the average of Λ electrons in every interval as this occurs only when the bit sequence is all 1's. In all other bit combinations, the average number of electrons required to be detected will be less than Λ .

The effect of the first DFE is to filter out the thermal noise. If J is large the number of errors e (errors in arrival time) will be large because in the first DFE the number of interfering symbols will increase. Even if PE for this DFE remains constant, increase in J will mean a corresponding increase in e . An arbitrary increase in J defeats the purpose of the first DFE which effectively filters out the thermal noise. Hence, $J = 2 \Lambda$ seems to be a reasonable choice. How actually the overall system performance changes with J can be answered only through simulation. Since simulation requires a large CPU time we have not done this but, have presented a heuristic argument.

CHAPTER 5

CONCLUSION

In this thesis we have considered the problem of optimal processing of received signal in an optical digital fibre communication system. We evaluated the likelihood function of the received signal and saw that the likelihood function is too complicated to yield a useful receiver. Thus, we made the assumptions that pulse-signal-to-noise ratio is very high (which holds when an avalanche diode is used) and electron emission times are quantized. The maximum likelihood function can then be mechanized using two Viterbi decoders in cascade. The first Viterbi decoder optimizes the familiar problem of detection of symbols in Gaussian noise and ISI. Implementation of Viterbi decoders with the present technology is almost ruled out. So we replace the two cascaded Viterbi decoders by two decision feedback equalizers. The first decision feedback equalizer is same as the receiver derived by Austin [13] and Salz [14]. In deriving the second decision feedback equalizer, we averaged the log-likelihood function instead of the likelihood function. To evaluate the averaged likelihood function, multiplications are to be done in 2^m parallel channels whereas only additions in m channels are required to evaluate the averaged log-likelihood function. Also, the memory size required reduces

from $2^{m-1}x2^m x^J$ to $2^{m-1}xmxJ$. Hence, we see that there is a considerable advantage in using the averaged log-likelihood function compared to the averaged likelihood function.

In Chapter 4 we have evaluated the performance of the proposed decision feedback equalizer. Since exact calculation of probability of error is difficult, we have calculated an upper bound on the probability of error, using Gram-Charlier series expansion method. We saw that the performance of the decision feedback equalizer considered is superior to a simple 'Integrate and Dump' receiver. Its performance is also better than a 'One Baud' receiver, but by less than 1 dB. Thus, when the impulse response of fibre is skewed to the first baud (as in the case of a short length fibre), the simpler 'One Baud' receiver can be used without too much loss of performance. The 'One Baud' receiver is actually a decision feedback equalizer in which ISI due to future symbols has been neglected.

The receiver considered here has two main drawbacks. One, the sampling rate, J, required is very high, and the other, high sensitivity of receiver to timing offsets. The sampling rate required is twice the average number of electrons emitted. This high sampling rate puts an upper limit on data rate which can be transmitted for a given receiver complexity. Also, the memory required increases exponentially with the number of interfering symbols. Hence the receiver derived is useful only when

the number of interfering symbols is not very large.

There is a large degradation in receiver performance with timing offset errors. Hence good synchronization schemes are required for reliable communication.

Some of the aspects of the present study which could be investigated further are techniques of optimizing equation (3.25) so that we do not have to make the assumption of quantized electron emission times. The second DFE will also change accordingly. The receiver proposed in this thesis has a drawback that sampling required is high which can be overcome by decreasing the sampling rate J and allowing q_j 's to take multiple values, instead of only binary values. This will result in complicating the first DFE and some loss of performance in the second DFE.

REFERENCES

1. Gagliardi, R.M. and Karp, S., 'Optical Communications', John Wiley and Sons, New York, 1976.
2. Van Trees, H., 'Detection, Estimation and Modulation Theory', vol. 1, John Wiley and Sons, New York, 1969.
3. Cartledge, J.C., 'Impulse Response of a Step Index Optical Fibre Excited by a Lambertian Source', Applied Optics, vol. 16, No.5, May 1977, pp 1311-1314.
4. Helstrom, C.W., Liu, J.W.S., Gordon, J.P., 'Quantum Mechanical Communication Theory', Proceedings of the IEEE, vol. 58, No.10, October 1970, pp 1578-1598.
5. Personick, S.D., 'Baseband Linearity and Equalization in Fibre Optic Digital Communication System', BSTJ , vol. 52, No. 7, September 1973, pp 1175-1194.
6. Bar-David, I., 'Communication Under the Poisson Regime', IEEE Transactions on Information Theory, IT-15, No.1, January 1969, pp 31-37.
7. Gagliardi, R.M. and Karp, S., 'M-ary Poisson Detection and Optical Communications', IEEE Transactions on Communication Technology, COM-17, No.2, April 1969, pp 208-216.
8. Personick, S.D., 'Receiver Design for Digital Fibre Optic Communication Systems', Part I and Part II, BSTJ, 52, No.6, July-August 1973, pp 843-886.

9. Messerschmitt, D.G., 'Minimum MSE Equalization of Digital Fibre Optic Systems', IEEE Transactions on Communications, COM-26, No.7, July 1978, pp 1110-1118.
10. Foschini, G.J., Gitlin, R.D. and Salz, J., 'Optimum Direct Detection for Digital Fibre Optic Communication Systems', BSTJ, vol. 54, No.8, October 1975, pp 1389-1430.
11. Jones, D.S., 'Asymptotic Behaviour of Integrals', SIAM Reviews, vol. 14, No.2, April 1972, pp 286-317.
12. Forney, G.D., 'Maximum-Likelihood Sequence Estimation of Digital Sequence in the Presence of Intersymbol Interference', IEEE Transactions on Information Theory, IT-18, No.3, May 1972, pp 363-378.
13. Austin, M.E., 'Decision-Feedback Equalization for Digital Communication Over Despersive Channels', MIT Research Laboratory of Electronics Technical Report 461 and Lincoln Laboratory Technical Report 437, August 11, 1967.
14. Salz, J., 'Optimum Mean-Square Decision Feedback Equalization', BSTJ, vol. 52, No.8, October 1973, pp 1341-1373.
15. Cariolaro, G., 'Error Probability in Digital Fibre Optic Communication System', IEEE Transactions on Information Theory, IT-24, No.2, March 1978, pp 213-221.
16. Digliotti, R., Luvison, A. and Pirani, G., 'Error Probability in Optical Fibre Transmission Systems', IEEE Transactions on Information Theory, IT-25, No.2, Mar 1979, pp 170-179.

17. Mansuripur, M., Goodman, J.W., Rawson, E.G. and Norton, R.E., 'Fibre Optic Receiver Error Rate Prediction Using the Gram-Charlier Series', IEEE Transactions on Communications, COM-28, No.3, Mar 1980, pp 402-407.